CHEMICAL ENGINEERING TRANSACTIONS
VOL. 113, 2024
A publication of AIDIC
The Italian Association of Chemical Engineering
Online at www.cetjournal.it
Guest Editors: Jeng Shiun Lim, Bohong Wang, Guo Ren Mong, Petar S. Varbanov

ISBN 979-12-81206-14-4; **ISSN** 2283-9216
DOI: 10.3303/CET24113042

Microstructural and Optoelectronic Characterization of Hybrid Lead Mixed Halide Films $CH_3NH_3PbI_{3-x}Cl_x$ Synthesized by Antisolvent Method

Nam Ngoc Lam[a], Tri Minh Le[b], Khoi Anh Tran[a], Dung Van Nguyen[a], Phung Thi Kim Le[c,*]

[a]Institute for Tropical Technology and Environmental Protection, 57A Truong Quoc Dung Street, Ward 10, Phu Nhuan District, Ho Chi Minh City, Vietnam
[b]Academy of Military Science and Technology, 17 Hoang Sam, Nghia Do Ward, Cau Giay District, Ha Noi City, VietNam
[c]CIRTech Institute, HUTECH University, Ho Chi Minh City, 700000, VietNam
ltk.phung@hutech.edu.vn

As the energy industry advances, perovskite solar cells emerge as potential successors in solar technology. Researchers are focusing on enhancing the stability and performance of hybrid lead halide perovskite $CH_3NH_3PbI_3$. One promising research direction is the use of hybrid lead mixed halide perovskite $CH_3NH_3PbI_{3-x}Cl_x$. Adding the chlorine element helps stabilize the perovskite's phase by reducing the lattice constant and improving the carrier diffusion length. In this study, we fabricated perovskite films $CH_3NH_3PbI_{3-x}Cl_x$ using the spin coating method combined with the antisolvent chlorobenzene. The synthesized films were dried at different temperatures. The microstructural and optoelectronic properties of the films were studied and evaluated by scanning electron microscopy, X-ray diffraction, energy-dispersive X-ray spectroscopy, and ultraviolet-visible spectroscopy. The Tauc plot method used ultraviolet-visible absorption spectroscopy to determine the energy bandgap of materials. Experimental results have shown that incorporating chlorobenzene leads to the formation of perovskite crystals with a uniform size. Controlling the annealing temperature allows for precise management of film growth during synthesis. The perovskite film annealed at 100 °C exhibits tetragonal structures, with a particle size of 500 nm and high surface coverage. This film demonstrates the capability to absorb light up to 820 nm, with a bandgap energy reaching 1.5 eV, indicating an improvement compared to traditional $CH_3NH_3PbI_3$ films. These results indicate the potential of this approach in producing perovskite films $CH_3NH_3PbI_{3-x}Cl_x$ as an absorber layer in solar cells, offering both high efficiency and cost effectiveness. In order to develop advanced solar panels that can supplant silicon cells, further investigation is imperative to enhance durability and manufacturing capabilities.

1. Introduction

Researchers are studying new solar cells with perovskite materials as substitutes for silicon solar cells (SSCs). The aim is to tackle cost, material, pollution concerns and conversion efficiency (Green et al., 2021). The energy conversion efficiency of perovskite solar cells (PSCs) is 18-22 %, similar to single crystal SSCs (20-22 %) and higher than multi crystal SSCs (15-20 %). The production cost of PCSs is lower due to simpler manufacturing processes and lower energy requirements, while SSCs need more costly processes for refining and crystal growth (Snaith, 2013). The impact of humid air and high temperatures makes PCSs stable for several years, while SSCs are stable for up to 25 y. This difference creates a challenge for PCSs commercial success, highlighting the importance of further research to improve their longevity and durability (Leijtens et al., 2015).
The $CH_3NH_3PbI_{3-x}Cl_x$ perovskite films, with their flexible crystal structure and easily tunable chemical and physical properties, are promising research materials for incorporation as absorber layers in next-generation solar cells. Due to their high charge mobility and long electron-hole diffusion length, even in polycrystalline layers (Stranks and Snaith, 2015), the utilization of $CH_3NH_3PbI_{3-x}Cl_x$ as a light-absorbing material helps mitigate

Paper Received: 25 May 2024; Revised: 30 July 2024; Accepted: 22 October 2024
Please cite this article as: Lam N.N., Le T.M., Tran K.A., Nguyen D.V., Phung T.K.L., 2024, Microstructural and Optoelectronic Characterization of Hybrid Lead Mixed Halide Films CH3NH3PbI3-xClx Synthesized by Antisolvent Method, Chemical Engineering Transactions, 113, 247-252 DOI:10.3303/CET24113042

charge recombination losses and reduce defect densities within the structure (Unger et al., 2014). Both $CH_3NH_3PbI_{3-x}Cl_x$ and $CH_3NH_3PbI_3$ share similarities in their crystal structures, exhibiting both cubic and tetragonal phases (Yu et al., 2014). The bandgap energy of $CH_3NH_3PbI_{3-x}Cl_x$ can be tailored from approximately 1.5 eV to 2.3 eV by adjusting the Cl^- and I^- ratio, offering control over the absorption and emission wavelengths of the material (Zhang et al., 2021).

Hybrid lead halide perovskites also have the disadvantage of being sensitive to environmental factors such as humidity, temperature, UV radiation and oxygen. Photo-generated holes with strong oxidizing properties will ionize $CH_3NH_3PbI_3$, leading to a series of redox reactions that accelerate the degradation of the perovskite, which primarily occurs at the $CH_3NH_3PbI_3/TiO_2$ interface. After exposure to UV radiation, electron-hole pairs are generated on the surface of the perovskite. O_2 will become superoxide (O_2^{*-}) by absorbing a photo-generated electron, leading to the ion reduction of the perovskite, forming CH_3NH_2, PbI_2, I_2, and H_2O (Bryant et al., 2016). Adjusting the halogen elements in the chemical composition enhances the stability of the perovskite structure against various environmental stressors. The combination of Br^- or Cl^- with I^- significantly improves the stability of $CH_3NH_3PbBr_{0.5}I_{2.5}$ and $CH_3NH_3PbI_{1.8}Cl_{1.2}$ perovskites. The two materials exhibited durability surpassing 2,000 h and 5,000 h, with respective efficiencies of 11.4 % and 12.4 % (Nguyên et al., 2022). This significantly enhances the performance and long-term reliability of optoelectronic devices.

Compared to the one step and two step spin coating methods, the spin coating method combined with antisolvents, using solvents with low boiling points and poor miscibility with the precursor solution, significantly affects the structure and optical properties of the perovskite layer through the crystallization process. The antisolvents flatten the surface of the perovskite films more effectively than conventional spin coating techniques, control the nucleation and crystal growth (Li et al., 2018), reduce crack formation, improve the uniformity and performance of the perovskite layer (Sun et al., 2021). The $CH_3NH_3PbI_3$ films, bricated using the spin coating method with ethyl acetate (EA) as an antisolvent, exhibit a surface morphology that is homogeneous, compact and flat. The grain size is approximately 450 nm. PSCs achieve the highest power conversion efficiency (PCE) of 17.4 % in ambient air with a relative humidity of 35 % (Zhang et al., 2019). Using 30 % antisolvent chlorobenzene (CB) in the perovskite precursor boosts PCE to 18.47 %, a 20 % increase from devices without antisolvent. CB contributes to sustaining the device performance for over 120 h in ambient conditions, with efficiency remaining at 72 %, while devices without CB drop to 11 % (Liu et al., 2020). Combining two antisolvents, ethyl acetate (EA) and isopropanol (IP), with a volume ratio of 1:0.06 during the spin coating process, resulted in a perovskite film with a smooth surface, exhibiting the smallest root mean square (R_q) surface roughness measured at 10.2 nm. The film displayed diffraction peaks at 14.2° and 28.1°, indicating crystals with (100) and (200) planes. Optical absorption spectra were measured up to 800 nm. The PSC achieved a PCE of 18.98 % with a stability of 90 % over 30 days under dry conditions (Liu et al., 2019). This outcome shows great potential for the advancement of perovskite solar cell technology in the upcoming years.

In this study, the precursor solution of perovskite $CH_3NH_3PbI_{3-x}Cl_x$ was synthesized with a molar ratio of CH_3NH_3I to $PbCl_2$ of 3:1. Perovskite films were fabricated using a spin coating method combined with the antisolvent chlorobenzene, followed by annealing at temperatures of 80 °C, 100 °C, and 150 °C. The morphology, structure, and optoelectronic properties of the films were subsequently investigated. The aim of this paper is to provide insights into the characteristics of $CH_3NH_3PbI_{3-x}Cl_x$ films, elucidating their potential for use in PSCs and other optoelectronic devices. The novelty of this study lies in the application of an antisolvent, which ensures the formation of $CH_3NH_3PbI_{3-x}Cl_x$ films with fewer defects, better uniformity, and cost efficiency compared to traditional spin coating techniques. Exploring the impact of annealing temperature offers the ability to manage the crystallization capacity and characteristics of the material.

2. Materials and Methods

2.1 Materials

Chlorobenzene (C_6H_5Cl, ≥ 99.9 %) and metylamine solution (CH_3NH_2, 40 % in methanol) were purchased from XiLong, China. Hydroiodic acid solution (HI, 55 % in water) was purchased from EG, China. Lead(II) chloride ($PbCl_2$, ≥ 99.5 %) was purchased from FuChen, China. N,N-dimethylformamide (DMF) ($HCON(CH_3)_2$, ≥ 99.5 %) was purchased from GhTech, China. Diethyl ether ($C_4H_{10}O$, ≥ 99.5 %) was purchased from DucGiang, VietNam. All materials were used as received.

2.2 Synthesis of perovskite films $CH_3NH_3PbI_{3-x}Cl_x$

CH_3NH_3I was prepared from CH_3NH_2 and HI at a 1:1 ratio as outlined in the publication (Mokhtar et al., 2018). The addition of HI to CH_3NH_2 was carried out slowly at 0 °C and stirred for 2 h in a nitrogen atmosphere. The solution was stirred at 60 °C until crystallization occurred and a gel-like mixture was formed. This mixture was rinsed with acetone 2-3 times and then dried at 60 °C for 24 h.

A precursor solution of $CH_3NH_3PbI_{3-x}Cl_x$ 1M was synthesized by the reaction of 2.3835 g of CH_3NH_3I with 1.3905 g of $PbCl_2$ (in a 3:1 ratio) in 5 ml of DMF. The solution was stirred at 60 °C for 30 min and subsequently filtered under vacuum using an 11 µm filter paper. To fabricate perovskite films, 40 µl of the precursor solution was uniformly distributed onto a 2.5x2.5 cm glass substrate positioned on the spin coater device Ossila L2001A3-E461-UK for a duration of 10 s. The films were spun at a rate of 1,000 rpm for 10 s and then at 4,000 rpm for 30 s. At 4,000 rpm, 20 µl of the antisolvent CB was deposited onto the surface. The glass substrate underwent annealing at temperatures of 80 °C, 100 °C and 150 °C for 1 h. The resulting materials were preserved in an environment of nitrogen and 35 % humidity.

2.3 Characterization of perovskite films $CH_3NH_3PbI_{3-x}Cl_x$

Surface morphology and elemental composition of the perovskite films were analyzed using scanning electron microscopy (SEM) and energy dispersive X-ray spectroscopy (EDX) (MIRA LMU). The crystal structure of the films was examined by X-ray diffraction (XRD) utilizing PANalytical (Aeris Mineral Edition) with Co Kα serving as the excitation source. The optoelectronic properties of the materials were investigated via ultraviolet-visible (UV-Vis) absorption spectroscopy (Jasco V–770 UV/VIS). From the absorption spectrum, the energy band gap (E_g) of the perovskite films can be determined using the Tauc plot method, was calculated using Eq(1) as follows:

$$(\alpha h\nu)^m = A(h\nu - E_g) \quad (1)$$

Where E_g is the band gap of the material, h is Planck's constant, A is constant, v is the frequency of light, α is absorption coefficient. The value of the coefficient m depends on the type of material (m = 2 for an indirect band gap and m = $\frac{1}{2}$ for direct band gap). The Tauc plot method involves plotting the recombination energy rate $(\alpha h\nu)^m$ against the photon energy (hv) of the incident light. A linear segment of the curve can be identified. By extending this linear segment until it intersects the horizontal axis, the value of the energy bandgap of the material can be derived.

3. Results and discussion

3.1 Surface morphology and elemental composition

Perovskite films are initially maintained in a metastable condition characterized by intricate internal crystalline phases finely adjusted by intermediate phases of polar solvents (Chen et al., 2021). The process of transitioning from a wet film to a stable perovskite structure is primarily instigated by the creation of a supersaturated environment resulting from solvent evaporation. Antisolvents like CB exhibit miscibility with DMF and play a key role in enhancing the rate of DMF evaporation. The treatment involving CB serves to stimulate heterogeneous nucleation by swiftly inducing supersaturation on the surface of the substrate during the spinning process (Shao et al., 2014). A critical aspect of this process is the application of thermal treatment, which aids in solvent evaporation, thereby facilitating the shift from intermediate phases to pure phases and exerting a significant impact on the morphological and structural characteristics of the films. The thermal treatment plays a pivotal role in eliminating residual stresses and internal defects, consequently refining the microstructure of the material. Figure 1a–c show the top-view SEM images of $CH_3NH_3PbI_{3-x}Cl_x$ perovskite films on a glass substrate, fabricated using spin coating with CB antisolvent and annealed at temperatures of 80 °C, 100 °C and 150 °C for 1 h.

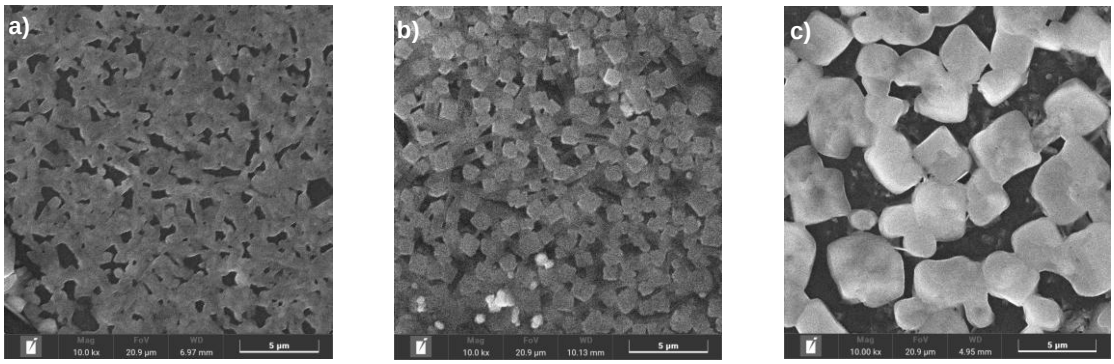

Figure 1: Top-view SEM images of $CH_3NH_3PbI_{3-x}Cl_x$ perovskite films annealed at (a) 80 °C, (b) 100 °C and (c) 150 °C

The average grain size of the perovskite films increased, along with their distribution, as the annealing temperature rose from 80 °C to 150 °C. It should be noted that excessive prolonged thermal annealing could result in film decomposition and jeopardize device stability due to the delicate nature of the perovskite structure. The swift evaporation of organic solvents triggered by elevated heating temperatures leads to rapid volume reduction, impeding solute diffusion and resulting in rough surfaces and cracking at grain boundaries (Wang et al., 2022). At a treatment temperature of 100 °C (Figure 1b), the film exhibits crystallization with particle sizes of about 500 nm, forming cuboids and polyhedral-like shapes, while the number of pinholes notably decreases, indicating a uniform distribution and better film quality compared to conditions at 80 °C and 150 °C. Figure 2 shows the EDX spectrum of the perovskite film annealed at 100 °C.

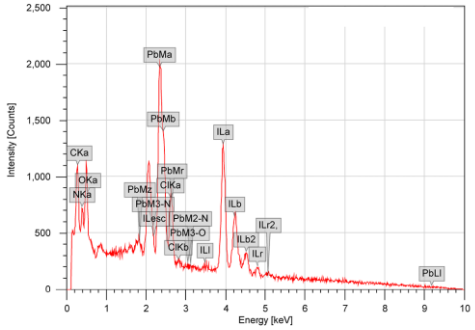

Figure 2: EDS analysis of $CH_3NH_3PbI_{3-x}Cl_x$ perovskite film annealed at 100 °C

Analysis of the spectrum indicates peaks corresponding to C, N, and Cl atoms emitting K-series X-rays, I atoms emitting L-series X-rays and Pb atoms emitting M-series X-rays. Hydrogen, being the lightest element with only one proton and one electron, does not emit characteristic X-rays in an energy range detectable. Mapping images of individual elements demonstrate their uniform distribution across the specimen's surface. The content of elements in the film is given in Table 1.

Table 1: The content of elements in $CH_3NH_3PbI_{3-x}Cl_x$ perovskite film annealed at 100 °C

Element	Mass, %	Atom, %
C	2.67	22.18
N	0.78	5.58
Cl	4.33	12.22
I	50.48	39.83
Pb	41.74	20.18
Total	100.00	100.00

3.2 Crystal structure

Figure 3 shows the XRD pattern of $CH_3NH_3PbI_{3-x}Cl_x$ perovskite film annealed at 100 °C. XRD analysis revealed a peak at 2θ = 12.6°, corresponding to the (001) plane of PbI_2, suggesting that $CH_3NH_3PbI_{3-x}Cl_x$ partially decomposed when exposed to air. Studying the structure of $CH_3NH_3PbI_{3-x}Cl_x$ perovskite films using the dip coating method also yielded similar results (Karim et al., 2019), demonstrating the sensitivity of hybrid perovskite materials to environmental conditions.

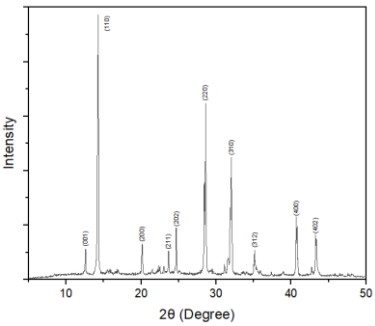

Figure 3: XRD pattern of $CH_3NH_3PbI_{3-x}Cl_x$ perovskite film annealed at 100 °C

High-intensity diffraction peaks were observed at 2θ values of 14.3°, 20.1°, 23.7°, 24.7°, 28.6°, 32.0°, 35.1°, 40.7° and 43.3°. These peaks correspond to the (110), (200), (211), (202), (220), (310), (312), (400) and (402) planes, respectively. The presence of these peaks confirms the tetragonal structure of the film with the I4/mcm space group. The observed diffraction pattern aligns with the crystallographic structure of $CH_3NH_3PbI_{3-x}Cl_x$, indicating that the material predominantly retains its tetragonal phase (Sewvandi et al., 2016).

3.3 Optoelectronic properties

By using Cl or swapping various anions within perovskite structures, novel structures with varying band gap energies can be produced, allowing for precise control of the band gap width to develop materials suitable for solar cell research and other optoelectronic applications, while also enhancing the performance of solar cells through the creation of perovskite composites capable of absorbing all wavelengths of light and minimizing electron back-transfer and recombination.

Figure 4a–b show the UV-Vis absorption spectrum and Tauc plot of $CH_3NH_3PbI_{3-x}Cl_x$ perovskite film annealed at 100 °C to evaluate the absorption ability of materials in the visible-infrared region. The perovskite film exhibits strong absorption capability in the near-infrared region with the absorption edge at approximately 820 nm, indicating a high potential for energy conversion and suitability for high-performance solar cells. Perovskite films fabricated using the antisolvent method, combining EA and IP, also yield similar results. The PSCs utilizing this material as an absorber layer achieve a PCE of 18.98 % (Liu et al., 2019).

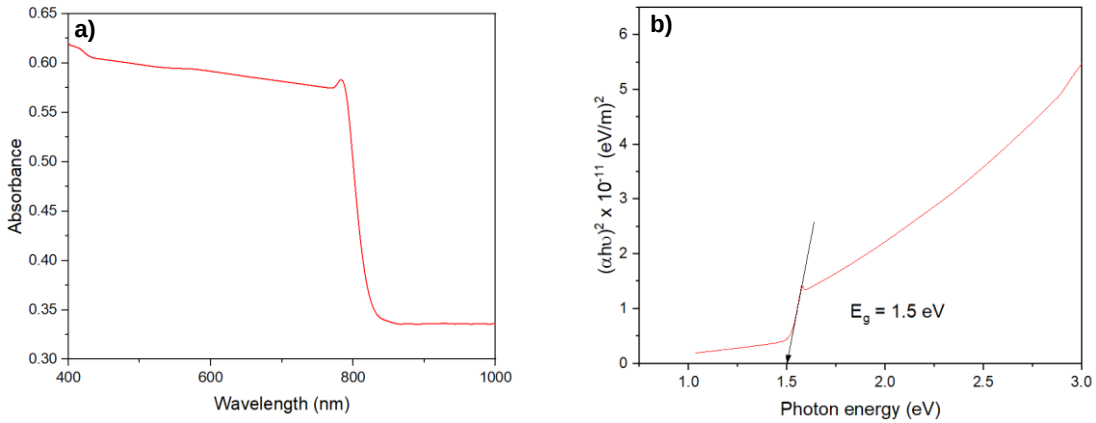

Figure 4: UV-Vis absorption spectrum (a) and Tauc plot (b) of $CH_3NH_3PbI_{3-x}Cl_x$ perovskite film annealed at 100 °C

Based on the Tauc plot (Figure 4b), the energy band gap of the material is determined to be 1.5 eV. Comparing this with the results for $CH_3NH_3PbI_3$ perovskite films, which have an absorption around 720 nm and a band gap energy of 1.56 eV (Mehra et al., 2022), the optoelectronic properties of the $CH_3NH_3PbI_{3-x}Cl_x$ films have improved significantly.

4. Conclusions

The $CH_3NH_3PbI_{3-x}Cl_x$ perovskite films were successfully synthesized using the spin coating method combined with the antisolvent chlorobenzene. This combined method effectively flattened the surface of the perovskite films more so than conventional spin coating techniques, enhancing the evaporation of the DMF solution and the crystallization of the material. In this study, the perovskite film annealed at 100 °C exhibited superior properties, including a tetragonal structure with the space group I4/mcm, a particle size of approximately 500 nm, an absorption capacity up to 820 nm and a band gap energy of 1.5 eV. The results also demonstrate that incorporating Cl into the composition improves the photovoltaic properties of the $CH_3NH_3PbI_3$ material and its potential for solar cell fabrication.

Acknowledgments

This work was funded by Academy of Military Science and Technology and supported from the Institute for Tropical Technology and Environmental Protection under grant number ĐTVCBT.80-3/VNĐMT.

References

Bryant D., Aristidou N., Pont S., Sanchez-Molina I., Chotchunangatchaval T., Wheeler S., Durrant J.R., Haque S.A., 2016, Light and oxygen induced degradation limits the operational stability of methylammonium lead triiodide perovskite solar cells, Energy & Environmental Science, 9(5), 1655-1660.

Chen S., Xiao X., Chen B., Kelly L.L., Zhao J., Lin Y., Toney M.F., Huang J., 2021, Crystallization in one-step solution deposition of perovskite films: Upward or downward?, Science Advances, 7(4), eabb2412.

Green M., Dunlop E., Hohl-Ebinger J., Yoshita M., Kopidakis N., Hao X., 2021, Solar cell efficiency tables (version 57), Progress in photovoltaics: research and applications, 29(1), 3-15.

Karim A.T., Hossain M., Khan M., Kamruzzaman M., Rahman M.A., Rahman M.M., 2019, Solution-processed mixed halide CH 3 NH 3 PbI 3− x Cl x thin films prepared by repeated dip coating, Journal of materials science, 54, 11818-11826.

Leijtens T., Eperon G.E., Noel N.K., Habisreutinger S.N., Petrozza A., Snaith H.J., 2015, Stability of metal halide perovskite solar cells, Advanced Energy Materials, 5(20), 1500963.

Li Y., Ji L., Liu R., Zhang C., Mak C.H., Zou X., Shen H.-H., Leu S.-Y., Hsu H.-Y., 2018, A review on morphology engineering for highly efficient and stable hybrid perovskite solar cells, Journal of Materials Chemistry A, 6(27), 12842-12875.

Liu J., Li N., Jia J., Dong J., Qiu Z., Iqbal S., Cao B., 2019, Perovskite films grown with green mixed anti-solvent for highly efficient solar cells with enhanced stability, Solar Energy, 181, 285-292.

Liu X., Xu C., Lee E.-C., 2020, Chlorobenzene-mediated control of crystallization in perovskite films for high-performance solar cells, ACS Applied Energy Materials, 3(12), 12291-12297.

Mehra S., Pandey R., Madan J., Sharma R., Goswami L., Gupta G., Srivastava A., 2022, Synthesis and Characterization of Mapbx3 (X= Cl, Br, I) Based Perovskites: Experimental and Scaps Simulation Correlation for Photovoltaic Applications.

Mokhtar M.Z., Chen Q., Lian Q., Lewis D.J., Saunders B.R., Walton A.S., Ke C.-R., Whittaker E., Hamilton B., Haque S., 2018, Decoupling structure and composition of ch3nh3pbi3–x br x films prepared by combined one-step and two-step deposition, ACS Applied Energy Materials, 1(10), 5567-5578.

Nguyên H.T.T., Hiền T.M., Nguyên H.L.T., Hải L.V., Hoàng N.T., 2022, Tổng hợp, phân tích tính chất và đánh giá độ bền của vật liệu perovskite hỗn hợp ion halogen (Cl, Br, I) và chế tạo pin mặt trời perovskite, Natural Sciences, 6(3), 2233-2240.

Sewvandi G.A., Kodera K., Ma H., Nakanishi S., Feng Q., 2016, Antiferroelectric nature of CH3NH3PbI3− xClx perovskite and its implication for charge separation in perovskite solar cells, Scientific reports, 6(1), 30680.

Shao Y., Xiao Z., Bi C., Yuan Y., Huang J., 2014, Origin and elimination of photocurrent hysteresis by fullerene passivation in CH3NH3PbI3 planar heterojunction solar cells, Nature communications, 5(1), 5784.

Snaith H.J., 2013, Perovskites: the emergence of a new era for low-cost, high-efficiency solar cells, The Journal of Physical Chemistry Letters, 4(21), 3623-3630.

Stranks S.D., Snaith H.J., 2015, Metal-halide perovskites for photovoltaic and light-emitting devices, Nature nanotechnology, 10(5), 391-402.

Sun J., Li F., Yuan J., Ma W., 2021, Advances in Metal Halide Perovskite Film Preparation: The Role of Anti-Solvent Treatment, Small Methods, 5(5), 2100046.

Unger E.L., Bowring A.R., Tassone C.J., Pool V.L., Gold-Parker A., Cheacharoen R., Stone K.H., Hoke E.T., Toney M.F., McGehee M.D., 2014, Chloride in lead chloride-derived organo-metal halides for perovskite-absorber solar cells, Chemistry of Materials, 26(24), 7158-7165.

Wang L., Liu G., Xi X., Yang G., Hu L., Zhu B., He Y., Liu Y., Qian H., Zhang S., 2022, Annealing engineering in the growth of perovskite grains, Crystals, 12(7), 894.

Yu H., Wang F., Xie F., Li W., Chen J., Zhao N., 2014, The role of chlorine in the formation process of “CH3NH3PbI3-xClx” perovskite, Advanced Functional Materials, 24(45), 7102-7108.

Zhang L., Sun C., He T., Jiang Y., Wei J., Huang Y., Yuan M., 2021, High-performance quasi-2D perovskite light-emitting diodes: from materials to devices, Light: Science & Applications, 10(1), 61.

Zhang Z., Luo X., Ding J., Zhang J., 2019, Preparation of high quality perovskite thin film in ambient air using ethylacetate as anti-solvent, Journal of Solid State Chemistry, 274, 199-206.